

Theory with Internal Degrees of Freedom: Merits and Limitations Demonstrated for the Potts Model

S. Heinrichs¹, W. Dieterich¹, P. Maass² and H. L. Frisch³

7. April 2003

Abstract

We present an extension of the density-functional theory (DFT) formalism for lattice gases to systems with internal degrees of freedom. In order to test approximations commonly used in DFT approaches, we investigate the statics and dynamics of occupation (density) profiles in the one-dimensional Potts model. In particular, by taking the exact functional for this model we can directly evaluate the quality of the local equilibrium approximation used in time-dependent density-functional theory (TDFT). Excellent agreement is found in comparison with Monte Carlo simulations. Finally, principal limitations of TDFT are demonstrated.

Keywords: density functional theory, local equilibrium approximation, non-equilibrium dynamics, potts model, lattice gas kinetics

¹Fachbereich Physik, Universität Konstanz, 78457 Konstanz, Germany

²Institut für Physik, Technische Universität Ilmenau, 98684 Ilmenau, Germany,
email: Philipp.Maass@tu-ilmenau.de

³Department of Chemistry, SUNY at Albany, Albany, New York 12222, U.S.A.

Density functional theory (DFT) and its time-dependent variant (TDFT) are powerful methods to derive phase diagrams and the kinetics of phase transformations [1, 2, 3] in condensed matter systems, in particular in the presence of confinement effects. Particularly useful are these theories for lattice systems [4, 5], allowing us to deal with the discrete nature of structures encountered e.g. in the description of metallic alloys, adsorbate layers, and complex pattern formation on atomic scales. This discrete DFT is more general than the ordinary DFT for fluid systems, being entailed by performing a proper continuum limit.

In the case where many ordered phases can coexist one is lead to include internal degrees of freedom into the DFT approach. As a prominent model we will consider in this work the q -state Potts model, which has a q -fold degenerate ground state [6]. The non-equilibrium dynamics of that model reflects the coarsening of domains following a quench from the disordered homogeneous phase to a system with long-range order seen in binary alloys, liquid crystals, magnetic bubbles, Langmuir films and soap bubbles [7]. The Potts model (in the limit $q \rightarrow 1$) is isomorphic to a site-bond percolation problem [8, 9] and for $q = 2$ it corresponds to the Ising model [10]. There are interesting experimental realizations for $q = 3$ (e.g. Kr on Graphite [11]), $q = 4$ and $q = \infty$ [12] (froths and metallic grains).

In this paper, based on the exact density functional for the one-dimensional q -state Potts model [13], we investigate the quality of various approximations often employed in DFT and TDFT. After presenting a general scheme for treating systems with internal degrees of freedom, we first consider the mean spherical approximation (MSA) for the equilibrium properties, and show how it compares with a mean-field approach and the exact solution. We then derive the TDFT [14] for the one-dimensional Potts model and, as an application, study the smoothening of an initial sharp-kink density profile. By comparison with Monte-Carlo simulations we show that the TDFT provides a significant improvement over kinetic mean field theory. Moreover, since in our case the TDFT is based on an exact density functional, the differences between the simulated and DFT results allow us to perform a specific test of the local equilibrium approximation used in the TDFT. Finally, we discuss principal limitations of the TDFT, where only the density profile is used to specify a non-equilibrium state of the system. This amounts to an incorrect account of correlations.

2 DFT for Lattice Gases with Internal Degrees of Freedom

We consider a lattice gas where each site i is either vacant ($x_i^\alpha = 0$ for all α) or singly occupied by a particle in one of q internal states. If state $\alpha \in \{1, \dots, q\}$ is realized, $x_i^\alpha = 1$ and $x_i^\beta = 0$ for $\beta \neq \alpha$. Occupation numbers therefore satisfy $x_i^\alpha x_i^\beta = x_i^\alpha \delta_{\alpha\beta}$. The Hamiltonian including two particle interactions $\Phi_{i,j}^{\alpha\beta}$ and site energies ϵ_i^α due to an external potential is given by

$$H = \frac{1}{2} \sum_{i \neq j} \sum_{\alpha, \beta} \Phi_{i,j}^{\alpha\beta} x_i^\alpha x_j^\beta + \sum_{i, \alpha} \epsilon_i^\alpha x_i^\alpha \quad (1)$$

The formal steps of DFT for fluids or lattice gases without internal degrees of freedom can be carried over to the case considered here. One arrives at a variational principle based on the functional for the grand canonical potential

$$\Omega[\mathbf{p}] = F[\mathbf{p}] + \sum_{i, \alpha} \tilde{\epsilon}_i^\alpha p_i^\alpha \quad (2)$$

where $\tilde{\epsilon}_i^\alpha = \epsilon_i^\alpha - \mu_\alpha$, μ_α being the chemical potential fixing the mean total occupation \bar{p}_α of state α , $\mathbf{p} = \{p_i^\alpha\}$ and $p_i^\alpha = \langle x_i^\alpha \rangle$ are the average occupation numbers. The free energy

$$F_{\text{id}}[\mathbf{p}] = \left[\sum_{i,\alpha} p_i^\alpha \ln p_i^\alpha + \sum_i \left(1 - \sum_\alpha p_i^\alpha \right) \ln \left(1 - \sum_\alpha p_i^\alpha \right) \right] \quad (3)$$

and an excess part $F_{\text{ex}}[\mathbf{p}]$ due to interactions (for convenience we set $k_B T = 1$). The equilibrium occupation is then obtained by minimizing $\Omega[\mathbf{p}]$ with respect to the p_i^α . The corresponding equations $\partial\Omega/\partial p_i^\alpha = 0$ determining the equilibrium profile are called structure equations. The minimum value of $\Omega[\mathbf{p}]$ is the grand-canonical potential at equilibrium.

Higher order derivatives of $\Omega[\mathbf{p}]$ with respect to the p_i^α taken at the equilibrium profile yield a hierarchy of direct correlation functions [2]. In particular, by differentiating the structure equation, the inhomogeneous Ornstein–Zernike equation

$$\tilde{c}_{ij}^{\alpha\beta} + \sum_{k,\gamma} \tilde{c}_{ik}^{\alpha\gamma} p_k^\gamma h_{kj}^{\gamma\beta} = h_{ij}^{\alpha\beta} \quad (4)$$

can be derived [4], which relates the direct correlation function $c_{i\alpha,j\beta}^{(2)} = -\partial^2 F_{\text{ex}}[\mathbf{p}]/\partial p_i^\alpha \partial p_j^\beta$ entering $\tilde{c}_{ij}^{\alpha\beta} = c_{i\alpha,j\beta}^{(2)} - \delta_{ij}/[1 - \sum_\mu p_i^\mu]$ to the pair correlation function $h_{ij}^{\alpha\beta} = g_{ij}^{\alpha\beta} - 1 = (1 - \delta_{ij}) \langle x_i^\alpha x_j^\beta \rangle / \langle x_i^\alpha \rangle \langle x_j^\beta \rangle$. In the limit $q = 1$ the known result for systems without internal degrees of freedom is recovered.

3 Application to the 1D Potts model

In the following, standard approximation schemes used in DFT are tested based on the one-dimensional Hamiltonian ($1 \leq i \leq M$)

$$H = \sum_{i,\alpha,\beta} v_i^{\alpha\beta} x_i^\alpha x_{i+1}^\beta + \sum_{i,\alpha} \tilde{\epsilon}_i^\alpha x_i^\alpha, \quad (5)$$

which for $v_i^{\alpha\beta} = V \delta_{\alpha\beta}$ reduces to the standard Potts model [6].

3.1 Exact density functional

For one-dimensional lattice gases with short range interactions, a general scheme for deriving exact density functionals based on Markov chains has recently been developed in [13]. This approach in particular provides an exact functional for the Potts model, which has been derived earlier by Percus [15]. The functional can be written as

$$\begin{aligned} \Omega[\mathbf{p}] = & \sum_{i=1}^M \left\{ \sum_{\alpha=1}^q \tilde{\epsilon}_i^\alpha p_i^\alpha + \sum_{\alpha,\beta=1}^q v_i^{\alpha\beta} \Gamma_i^{\alpha\beta} + \right. \\ & + \sum_{\beta} \left[\sum_{\alpha} \Gamma_i^{\alpha\beta} \log \frac{\Gamma_i^{\alpha\beta}}{p_{i-1}^\beta} + \left(p_{i-1}^\beta - \sum_{\alpha} \Gamma_i^{\alpha\beta} \right) \log \left(1 - \frac{\sum_{\alpha} \Gamma_i^{\alpha\beta}}{p_{i-1}^\beta} \right) \right] \\ & + \sum_{\alpha} \left(p_i^\alpha - \sum_{\beta} \Gamma_i^{\alpha\beta} \right) \log \left(\frac{p_i^\alpha - \sum_{\beta} \Gamma_i^{\alpha\beta}}{1 - \sum_{\beta} p_{i-1}^\beta} \right) \\ & \left. + \left(1 - \sum_{\beta} (p_{i-1}^\beta + p_i^\beta) + \sum_{\alpha,\beta} \Gamma_i^{\alpha\beta} \right) \log \left(1 - \frac{\sum_{\beta} p_i^\beta - \sum_{\alpha,\beta} \Gamma_i^{\alpha\beta}}{1 - \sum_{\beta} p_{i-1}^\beta} \right) \right\}, \end{aligned} \quad (6)$$

where the correlators

$$\Gamma_i^{\alpha\beta} = \langle x_{i-1}^\alpha x_i^\beta \rangle \quad (7)$$

the correlator equations [13]

$$\Gamma_i^{\alpha\beta} = e^{-v_i^{\alpha\beta}} \frac{(p_i^\alpha - \sum_\gamma \Gamma_i^{\alpha\gamma})(p_{i-1}^\beta - \sum_\delta \Gamma_i^{\delta\beta})}{1 - \sum_\gamma (p_{i-1}^\gamma + p_i^\gamma) + \sum_{\gamma,\delta} \Gamma_i^{\delta\gamma}}. \quad (8)$$

A simpler expression for the functional is obtained if the vacancies are considered as an additional Potts state with index $\alpha = 0$ (and $v_i^{00} = v_i^{0\beta} = 0$), whereby the lengthy entropic part reduces to $\sum_{i=1}^M \sum_{\alpha,\beta=0}^q \Gamma_i^{\alpha\beta} \log(\Gamma_i^{\alpha\beta}/p_i^\alpha)$. In the fully occupied case ($\sum_\alpha x_i^\alpha = 1$) the solution of eqs. (8) requires a careful limiting procedure by letting the vacancy concentration go to zero.

The structure equations read

$$e^{-\tilde{\epsilon}_i^\alpha} = \frac{(1 - \sum_\beta p_i^\beta) \left(p_i^\alpha - \sum_\gamma \Gamma_i^{\alpha\gamma} \right) \left(p_i^\alpha - \sum_\delta \Gamma_{i+1}^{\delta\alpha} \right) \frac{1}{p_i^\alpha}}{\left(1 - \sum_\beta (p_{i-1}^\beta + p_i^\beta) + \sum_{\gamma,\delta} \Gamma_i^{\delta\gamma} \right) \left(1 - \sum_\beta (p_i^\beta + p_{i+1}^\beta) + \sum_{\gamma,\delta} \Gamma_{i+1}^{\delta\gamma} \right)}. \quad (9)$$

By solving this equation numerically we obtain the exact density profiles. (For the example of eq. (15), results are shown in Fig. 1.)

3.2 Mean spherical approximation (MSA)

In the following the excess density functional will be expanded around a homogeneous reference state, $p_i^\alpha = \bar{p}_\alpha$ [16]. For simplicity, we here consider the standard Potts case $v_i^{\alpha\beta} = V\delta_{\alpha\beta}$, and set $\bar{p}_\alpha = \bar{p}$ for all α .

Defining $\Delta p_i^\alpha = p_i^\alpha - \bar{p}$, $\Delta\Omega[\mathbf{p}] = \Omega[\mathbf{p}] - \Omega[\{\bar{p}\}]$, etc., we can write

$$\Delta\Omega[\mathbf{p}] = \Delta F_{\text{id}}[\mathbf{p}] + \Delta F_{\text{ex}}[\mathbf{p}] + \sum_{i,\alpha} \tilde{\epsilon}_i^\alpha \Delta p_i^\alpha. \quad (10)$$

When retaining only terms up to second order in the excess free energy functional, we find

$$\Delta F_{\text{ex}}[\mathbf{p}] = - \sum_{i,\alpha} c^{(1)}(\bar{p}) \Delta p_i^\alpha - \frac{1}{2} \sum_{i,\alpha,j,\beta} c_{\alpha\beta}^{(2)}(|i-j|, \bar{p}) \Delta p_i^\alpha \Delta p_j^\beta, \quad (11)$$

where $c^{(1)}(\bar{p})$ can be subsumed into the chemical potential. For our choice of interactions with translational symmetry, $g_{ij}^{\alpha\beta} = g_{\alpha\beta}(|i-j|)$, and the direct correlation function $c_{i\alpha,j\beta}^{(2)}$ can be split into two parts,

$$c_{i\alpha,j\beta}^{(2)} = \delta_{\alpha\beta} c_1(|i-j|) + (1 - \delta_{\alpha\beta}) c_2(|i-j|). \quad (12)$$

where in the MSA approximation,

$$c_1(|l|) = \begin{cases} -V, & |l| = 1 \\ 0, & |l| \geq 2 \end{cases} \quad \text{and} \quad c_2(|l|) = 0 \quad \text{for} \quad |l| \geq 1 \quad (13)$$

and $g_{\alpha\beta}(l=0) = 0$. The two unknowns $c_1(0)$ and $c_2(0)$ are found using the Ornstein–Zernike equation (4), which yields

$$\begin{aligned} c_1^{(2)}(0) &= \frac{1 + \bar{p} - q\bar{p}}{\bar{p}(1 - q\bar{p})} - \frac{1}{q} [A + (q-1)B] \\ c_2^{(2)}(0) &= \frac{1}{1 - q\bar{p}} - \frac{1}{q} [A - B] \\ \text{with} \quad A &= \frac{\sqrt{1 + [2V\bar{p}(1 - q\bar{p})]^2}}{\bar{p}(1 - q\bar{p})}, \quad B = \frac{\sqrt{1 + (2V\bar{p})^2}}{\bar{p}}. \end{aligned} \quad (14)$$

states $\alpha = 2, \dots, q$ and alternating external energies for the Potts state $\alpha = 1$,

$$\epsilon_i^\alpha = \begin{cases} \epsilon, & i \text{ even and } \alpha = 1 \\ 0, & \text{otherwise} \end{cases} \quad (15)$$

and assume $\mu_\alpha = \mu$ independent of α . Due to the symmetry of this external potential, each occupation number p_i^α is equal to one of the four representatives $p_0^1, p_0^2, p_1^1, p_1^2$, and the mean particle density per site is

$$\bar{n} = \frac{1}{2} [p_0^1 + p_1^1 + (q-1)(p_0^2 + p_1^2)]. \quad (16)$$

We consider the functional

$$\begin{aligned} \Psi[\mathbf{p}] &\equiv \frac{1}{M} (\Delta\Omega[\mathbf{p}] + F_{\text{id}}[\bar{p}]) \\ &= \frac{1}{2} [p_0^1 \ln p_0^1 + p_1^1 \ln p_1^1 + (q-1) (p_0^2 \ln p_0^2 + p_1^2 \ln p_1^2) \\ &\quad + (1 - p_0^1 - (q-1)p_0^2) \ln (1 - p_0^1 - (q-1)p_0^2) \\ &\quad + (1 - p_1^1 - (q-1)p_1^2) \ln (1 - p_1^1 - (q-1)p_1^2)] \\ &\quad - \frac{1}{4} \left[c_1(0) \left((\Delta p_0^1)^2 + (\Delta p_1^1)^2 + (q-1) ((\Delta p_0^2)^2 + (\Delta p_1^2)^2) \right) \right. \\ &\quad \left. + c_2(0)(q-1) \{ 2 (\Delta p_0^1 \Delta p_0^2 + \Delta p_1^1 \Delta p_1^2) \right. \\ &\quad \left. + (q-2) ((\Delta p_0^2)^2 + (\Delta p_1^2)^2) \} \right. \\ &\quad \left. - 4V (\Delta p_0^1 \Delta p_1^1 + (q-1) \Delta p_0^2 \Delta p_1^2) \right] \\ &\quad + \frac{1}{4} \epsilon [p_0^1 - p_1^1 - (q-1)(p_0^2 + p_1^2) + 2(q-1)\bar{p}] \\ &\quad - \mu_{\text{eff}} \left[\frac{1}{2} (p_0^1 + p_1^1 + (q-1)(p_0^2 + p_1^2)) - \bar{n} \right]. \end{aligned} \quad (17)$$

with $\mu_{\text{eff}} = \mu - \epsilon/2 + c^{(1)}(\bar{p})$. The structure equations are obtained by setting the derivatives of $\Psi[\mathbf{p}]$ with respect to $p_0^1, p_0^2, p_1^1, p_1^2$ equal to zero. These equations are solved numerically subject to a fixed \bar{n} in eq. (16) (which is equivalent to $\partial\Psi/\partial\mu_{\text{eff}} = 0$). Ordinary mean field theory can be recovered from the functional by setting $c_1(0) = c_2(0) = 0$.

In Fig. 1 the occupation numbers for the MSA approximation and the mean field theory are compared with the exact results based on eq. (9). Without interactions ($V = 0$) the external potential yields mean occupation numbers $p_0^1 < p_1^1 = p_1^2 < p_0^2$, $p_0^1 = e^{-\epsilon} p_0^2$. When a repulsive interaction $V > 0$ is switched on, the fact that $p_1^1 > p_1^2$ induces an increasing occupation difference. For larger q this effect becomes less pronounced due to the increasing contribution of the entropy to the free energy per site.

As expected, the MSA is an improvement over the simple mean field approximation especially for higher values of the interaction parameter and high overall densities \bar{n} . Moreover, the quality of the MF-results can be shown to improve when ϵ is decreased. A notable result is the improvement of the two approximations for larger q , reflecting the fact that mean-field descriptions should become exact in the limit $q \rightarrow \infty$.

3.3 Kinetics of density profiles

So far we have considered density profiles at equilibrium. In order to account for the time evolution of non-equilibrium profiles we will make use of the local equilibrium approximation

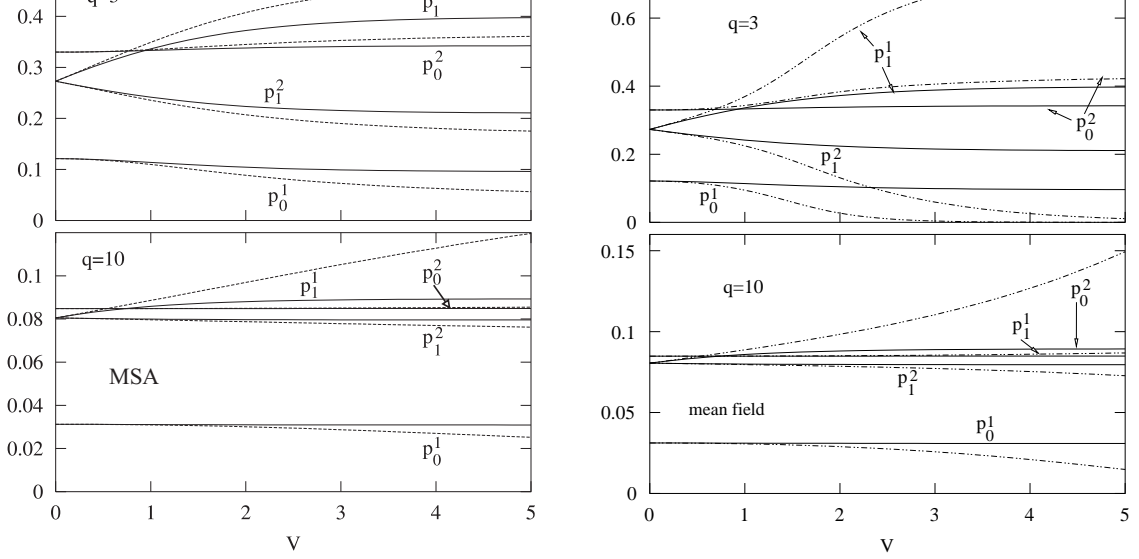


Figure 1: Exact occupation numbers versus interaction strength V , see section 3.1 (solid lines) for $\bar{n}=0.8$ and $\epsilon = 1$, and comparison with the DFT results in the MSA approximation (dashed lines) and mean field results (dashed-dotted lines).

for the probability distribution $P(\mathbf{x}, t)$ to find a configuration $\mathbf{x} = \{x_i^\alpha\}$ at time t . In this time-dependent density functional theory (TDFT) [5, 3], the deviations of $P(\mathbf{x}, t)$ from the Boltzmann equilibrium distribution are described by a one-particle time-dependent effective potential $h_i^\alpha(t)$,

$$P(\mathbf{x}, t) = \frac{1}{Z(t)} \exp \left[-H(\mathbf{x}) - \sum_{i,\alpha} h_i^\alpha(t) x_i^\alpha \right]. \quad (18)$$

The effective potential is the unique potential, which yields the instantaneous density profile $p_i^\alpha(t)$ according to the equilibrium DFT. Accordingly, the unknown field \mathbf{h} in eq. (18) can be determined by the ‘‘structure equation’’ $h_i^\alpha(t) = -\partial \Omega[\mathbf{p}] / \partial p_i^\alpha$ with $\Omega[\mathbf{p}]$ from eq. (2). It is then clear that in this approach all equilibrium relations between occupational correlators $\langle x_i^\alpha x_j^\beta \dots \rangle$ and the density \mathbf{p} also apply at each time instant to the non-equilibrium situation [in particular eq. (8)].

To test the quality of the TDFT, we consider a lattice with all sites being occupied ($\bar{n} = 1$) and a nonconserved dynamics, where a given Potts state α on lattice site i can change to any other state $\beta \neq \alpha$ with a rate $w_i^{\alpha\beta}(\mathbf{x})$ that depends on the current state \mathbf{x} due to interactions. From the master-equation describing this stochastic process, we derive the equation of motion for the occupation profile,

$$\frac{dp_i^\alpha}{dt} = \sum_\beta \langle (x_i^\beta - x_i^\alpha) w_i^{\alpha\beta} \rangle_t \quad (19)$$

where $\langle \dots \rangle_t$ denotes an average with respect to the non-equilibrium distribution $P(\mathbf{x}, t)$. For the rates we choose a generalized Glauber form,

$$\begin{aligned} w_i^{\alpha\beta}(\mathbf{x}) &= \left(1 - \tanh \left[(x_{i-1}^\beta x_i^\beta - x_{i-1}^\alpha x_i^\alpha) V / 2 \right] \right) \\ &\times \left(1 - \tanh \left[(x_{i+1}^\beta x_i^\beta - x_{i+1}^\alpha x_i^\alpha) V / 2 \right] \right), \end{aligned} \quad (20)$$

which satisfies the condition of detailed balance [18].

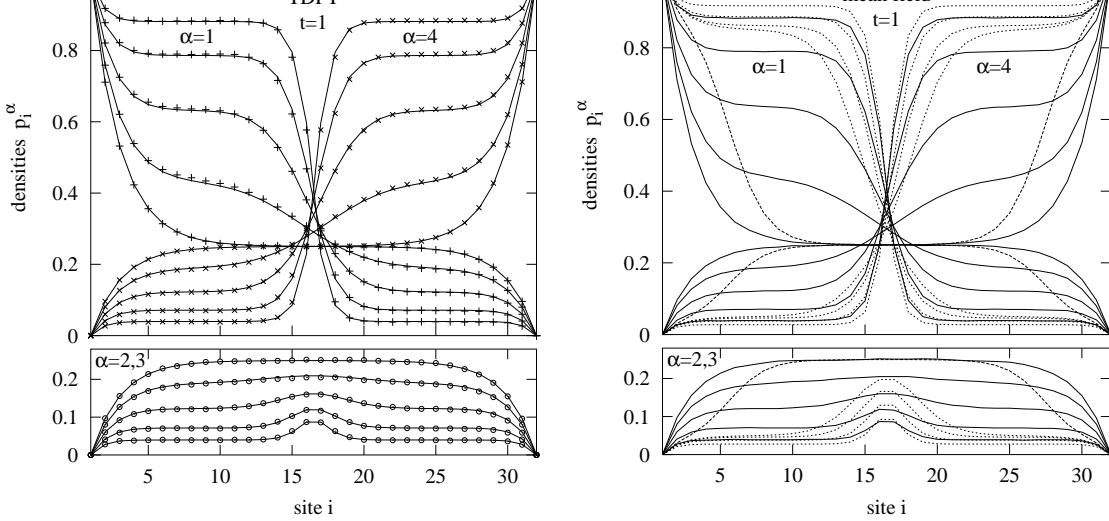


Figure 2: (a) Comparison of the evolution of an initial kink profile calculated using TDFT (lines) with monte carlo simulations (points) for a system with 32 particles, $q = 4$ and $V = -2$. Results are shown for $t = 1, 2, 4, 8$ and the equilibrium density. (b) Comparison of mean field theory (dotted lines) with the simulations (solid lines) for the same system as shown in (a). The mean field equilibrium solution is shown as the dashed line.

When substituting eq. (20) in (19) further evaluation is made possible by noting that the factor in front of $V/2$ in the argument of \tanh is always $-1, 0$ or 1 , so that it can be taken out from the \tanh function. With the help of the Markov property, three-point correlators can exactly be reduced to two-point correlators, e.g. $\langle x_{i-1}^\alpha x_i^\beta x_{i+1}^\gamma \rangle = \Gamma_i^{\alpha\beta} \Gamma_{i+1}^{\beta\gamma} / p_i^\beta$. After some algebra we then find

$$\begin{aligned}
 \frac{dp_i^\alpha}{dt} = & 1 - qp_i^\alpha + \tanh(V/2) \left[2p_i^\alpha - p_{i-1}^\alpha - p_{i+1}^\alpha \right. \\
 & + \sum_\beta \left(\Gamma_i^{\beta\beta} - \Gamma_i^{\alpha\alpha} + \Gamma_{i+1}^{\beta\beta} - \Gamma_{i+1}^{\alpha\alpha} \right) \left. \right] \\
 & + \tanh^2(V/2) \sum_\beta \left[\frac{1}{p_i^\beta} (\Gamma_i^{\alpha\beta} - \Gamma_i^{\beta\beta}) (\Gamma_{i+1}^{\beta\alpha} - \Gamma_{i+1}^{\beta\beta}) \right. \\
 & \left. - \frac{1}{p_i^\alpha} (\Gamma_i^{\beta\alpha} - \Gamma_i^{\alpha\alpha}) (\Gamma_{i+1}^{\alpha\beta} - \Gamma_{i+1}^{\alpha\alpha}) \right]. \quad (21)
 \end{aligned}$$

Equations (21) together with the correlator equations (8) form a complete set of equations for the time evolution of density profiles and can be solved numerically for a given initial condition.

As an example, we consider an initially sharp kink profile at time $t = 0$, where the left part of the system is in Potts state $\alpha = 1$ and the right part in Potts state $\alpha = q$ with fixed boundary sites $i = 1$ and M in Potts states $\alpha = 1$ and q , i.e. $x_1^\alpha = \delta_{\alpha,1}$ and $x_M^\alpha = \delta_{\alpha,q}$. In Figure 2a we compare the time evolution of the profile with the results from continuous-time Monte-Carlo simulations. The agreement is excellent for all times until for large times the TDFT solution and the simulations both yield the correct equilibrium profile. In order to obtain this agreement, it was necessary to adjust the time scale according to $t_{\text{TDFT}} = 0.85 t_{\text{MC}}$. The significant improvement over a simple mean-field treatment corresponding to factorization of all correlators in eq.(21), i.e. $\Gamma_i^{\alpha\beta} = p_{i-1}^\alpha p_i^\beta$, etc., can be seen by comparing Fig. 2a with Fig. 2b. The mean-field approximation is insufficient from

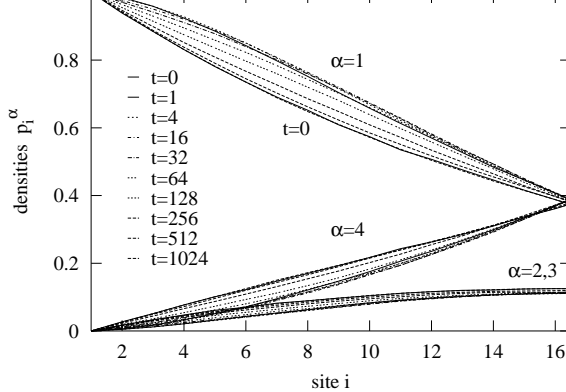


Figure 3: Evolution of a density profile starting from the equilibrium density, but with non-equilibrium correlators (see text) for $V = -4$ and $q = 4$. The system quickly reaches the state with maximum deviation from the equilibrium density at $t \approx 1$ and then relaxes to the original equilibrium density profile. Only the left half of the system is shown.

the beginning and does not provide the correct equilibrium profile for long times.

3.4 Basic Limitations of TDFT

Since in the kinetic equation of the TDFT only the densities (mean occupation numbers) enter, the TDFT can not distinguish between states with the same density profile but different correlations. As a consequence, the time evolution of a non-equilibrium state with the equilibrium density profile cannot be captured. This issue may become important when considering memory effects in systems with slow relaxations, as for example glassy systems. The observables used to characterize the thermodynamic states of such systems (as e.g. density) may have equal values initially, but very different time evolutions depending on the systems' history.

To illustrate this principal failure of the TDFT, we generate states of the Potts model with the same mean occupation numbers but different correlations for the same system as in the previous chapter. To achieve this, we first determine the equilibrium profile p_i^α for a system with interactions from the structure equations (9). This profile is also the equilibrium profile for a system without interactions ($V = 0$) and external potential $\epsilon_i^\alpha = -\log p_i^\alpha$. Hence by taking the equilibrium state of the non-interacting system as initial non-equilibrium state for the interacting system, we can study by Monte-Carlo simulations the time development of a density profile that according to TDFT cannot change.

Figure 3 shows the effect for $V = -4$ and $q = 4$. Although the mean occupation numbers at time $t = 0$ are the same as in the equilibrium state reached for $t \simeq 1024$, there is a pronounced change in the occupation profile at intermediate times. These changes are due to the fact that in the initial state the correlations between occupation numbers are not the equilibrium ones. The configurations with large statistical weights in the initial state exhibit stronger short-wavelength fluctuations and in order for the correlations to build up, the system has to pass through intermediate states with a non-equilibrium profile.

3.5 Acknowledgments

We gratefully acknowledge financial support by the Sonderforschungsbereich 513 of the Deutsche Forschungsgemeinschaft.

- [1] H. Löwen, Phys. Reports **237**, 249 (1994).
- [2] R. Evans, Adv. Phys. **28**, 143 (1979).
- [3] J.-F. Gouyet, M. Plapp, W. Dieterich, and P. Maass, Adv. Phys., in press
- [4] M. Nieswand, W. Dieterich, and A. Majhofer, Phys. Rev. E, **47**, 718 (1993).
- [5] D. Reinel, W. Dieterich, J. Chem. Phys. **104**, 5234 (1996); H. P. Fischer, J. Reinhard, W. Dieterich, J. F. Gouyet, P. Maass, A. Majhofer, and D. Reinel, J. Chem. Phys. **108**, 3028 (1998).
- [6] R. B. Potts, Proc. Cambridge Philos. Soc. **48**, 106 (1952); for a review, see F. Y. Wu, Rev. Mod. Phys. **54**, 235 (1982).
- [7] C. Sire and S. M. Majumdar, Phys. Rev. E **52**, 244 (1995) and references therein.
- [8] P. W. Kasteleyn and C. M. Fortuin, J. Phys. Soc. Japan Suppl. **16**:11 (1969); T. Lubensky in “Ill Condensed Matter”, eds. R. Balian, R. Mynard and G. Toulouse, North-Holland, Amsterdam, 1979.
- [9] A. Coniglio and W. Klein, J. Phys. A **13**, 2775 (1980).
- [10] P. M. Chaikin and T. C. Lubensky, “Principles of condensed matter physics”, Cambridge University Press, 1995, p. 256.
- [11] R. J. Birgeneau and P. M. Horn, Science **232**, 329 (1986).
- [12] see e.g. J. A. Glazier, M. P. Anderson and G. S. Grest, Philos. Mag. B **59**, 293 (1989) and references therein.
- [13] J. Buschle, P. Maass, and W. Dieterich, J. Phys. A Math. Gen. **33**, L41 (2000).
- [14] For the application of TDFT to the one-dimensional Ising model, see M. Kessler, W. Dieterich, H. L. Frisch, J. F. Gouyet, and P. Maass, Phys. Rev. E **65**, 066112 (2002).
- [15] J. K. Percus, J. Math. Phys. **23**, 1162 (1982).
- [16] An alternative possibility would be to choose a reference state being homogeneous in space but inhomogeneous in the space of Potts states, i.e. $p_i^\alpha = \bar{p}_\alpha$. In certain applications this might be advantageous. For simplicity, however, we will not consider this case here.
- [17] J. Reinhard, W. Dieterich, P. Maass, and H. L. Frisch, Phys. Rev. E **61**, 422 (2000).
- [18] For a Hamiltonian H that is decomposable into independent parts, $H = \sum_i H_i$, the generalized Glauber rate w_{ab} for a transition from an initial state a to a final state b in the form $w_{ab} = \prod_i \{1 - \tanh[(H_i^{(b)} - H_i^{(a)})/2]\}$ always satisfies the condition of detailed balance.